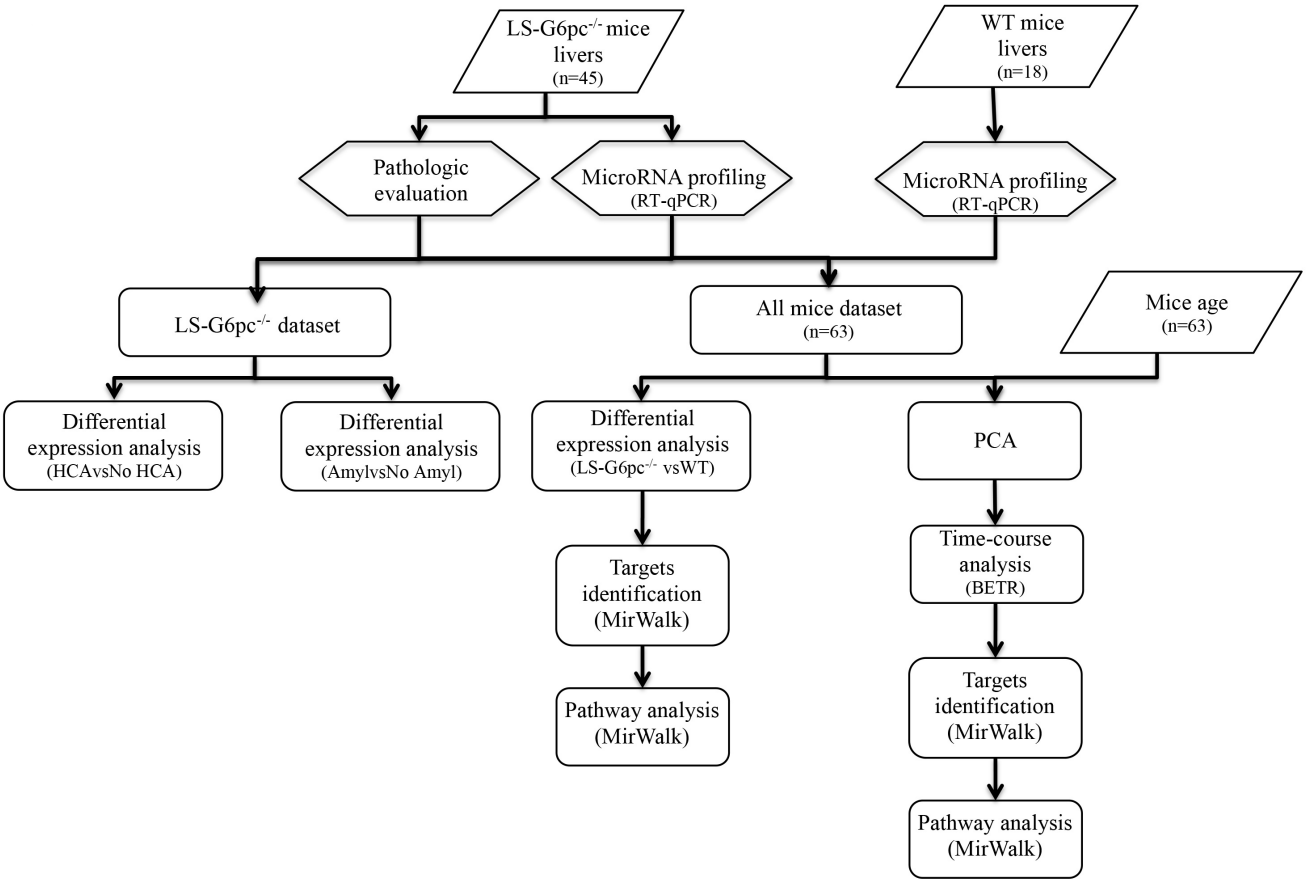

Fig. S1. Schematic representation of the whole bioinformatic strategy used in the study. The microRNA representation profile of 45 LS-G6pc$^{-/-}$ and 18 WT mouse plasma exosomes was measured by ViiA 7 RT-qPCR. Pathological evaluation of the livers assessed the presence of hepatic adenomas and/or amyloidosis within the entire set of mice samples. Differential expression analysis assessed any significant modulation of the Exo-miR between groups of LS-G6pc$^{-/-}$ and WT mice, LS-G6pc$^{-/-}$ mice characterized by the presence\absence of hepatic adenomas, or LS-G6pc$^{-/-}$ mice characterized by the presence/absence of amyloidosis. The representation profile of LS-G6pc$^{-/-}$ and WT mice over 6 distinct age groups was compared using BETR method. Analysis identified age-dependent modulated Exo-miR whose targets were identified using MirWalk tool. Pathway analysis on these targets identified the most significantly altered biological processes and pathways.

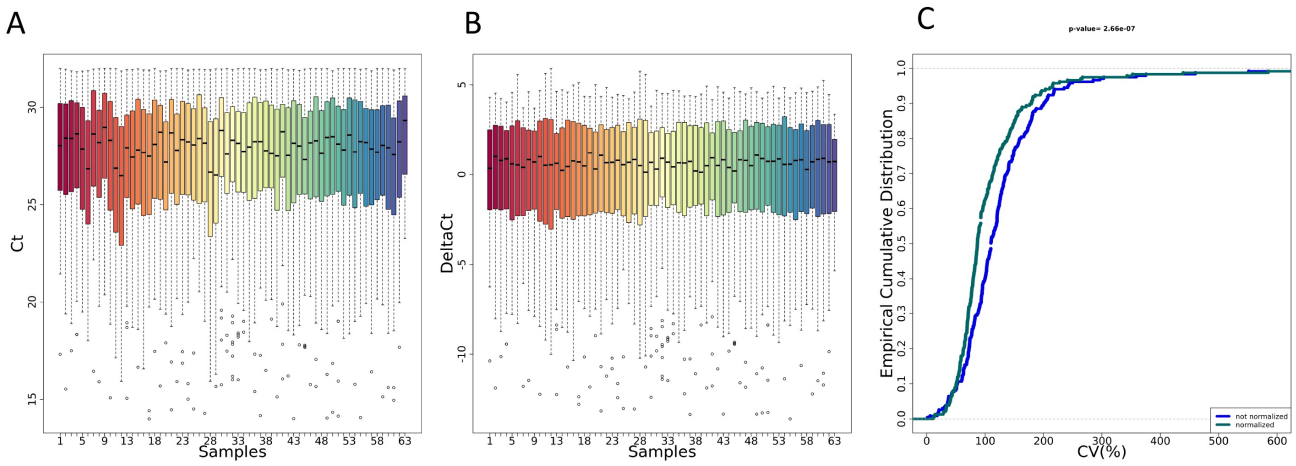

Fig. S2. Qualitative and quantitative assessment of the noise reduction for LS-G6pc$^{-/-}$ and WT mice data

The box plots reported in panels A and B show the distribution of Ct and delta Ct values for every samples before and after data normalization, respectively. The plot reported in panel C show the ECDFs (y axis) and the coefficient of variation (CV) for every samples before (blue line) and after (Green line) data normalization. Kolmogorov-Smirnov test assessed the significance of the separation between the curves and the p-value is reported on top of the plot. P-value lower than 0.05 is considered significant. Global mean was used to normalize the data.

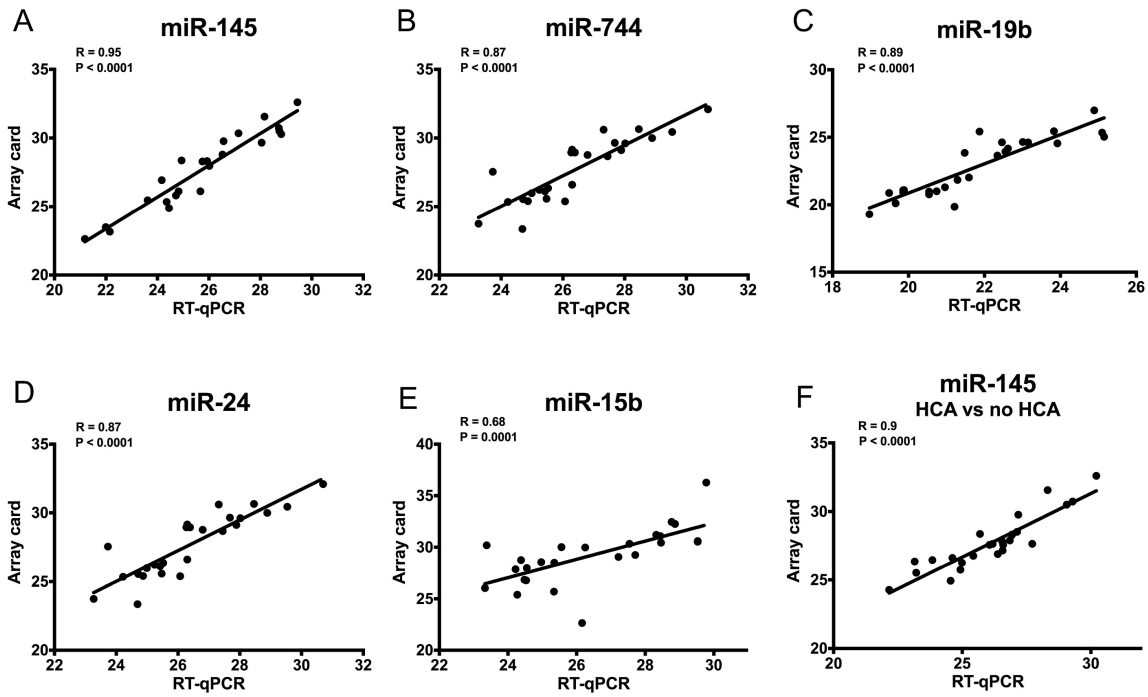

Fig. S3. Scatter plots of Ct values measured by RT-qPCR and Array card

A scatter plot showing correlation between the expression values measured by RT-qPCR and Array card on LS-G6pc$^{-/-}$ and WT mice samples is depicted for a selection of significant Exo-miR**.** Each point is the Ct value of a sample measured by RT-qPCR and Array card. Correlation is assessed by Pearson method. Linear regression line is superimposed to the points within each plot. Pearson correlation and p-value are reported in the top left side of the plots.

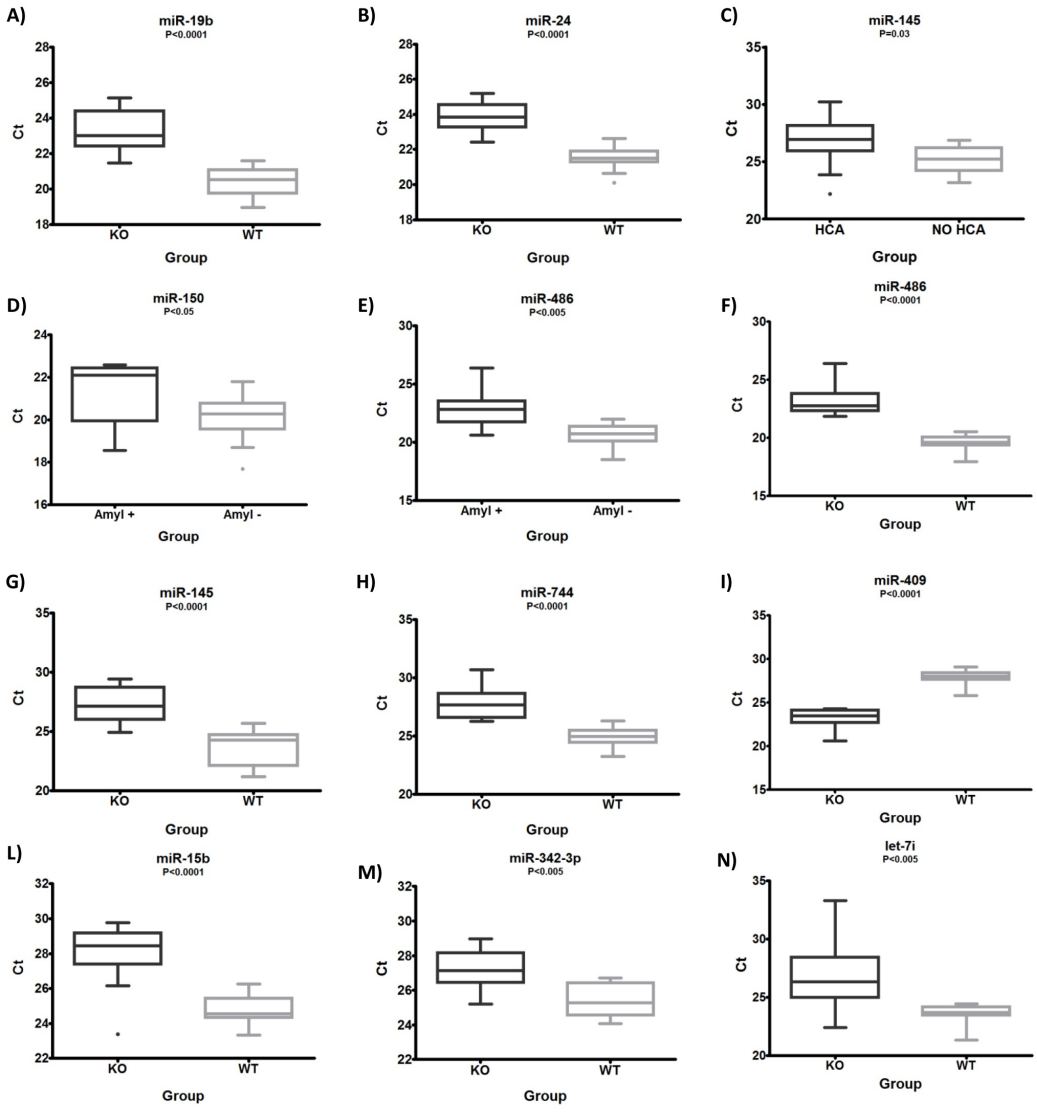

Fig. S4. Box plots of Ct values measured by RTqPCR between LS-G6pc$^{-/-}$ and WT mice; LS-G6pc$^{-/-}$ mice with and without amyloidosis; LS-G6pc$^{-/-}$ mice with and without adenoma.

Box-plots showing the differential expression between LS-G6pc$^{-/-}$ and WT mice, between LS-G6pc$^{-/-}$ mice with and without amyloidosis and between LS-G6pc$^{-/-}$ mice with and without adenoma are depicted for a selection of significant Exo-miR. Ct values were measured by RTqPCR. Statistical significance of the difference is assessed by unpaired t-test. P values and the name of the microRNA are reported on the top of each plot.

Table S1. Enrichment of GO biological processes and KEGG pathways in LS-G6pc$^{-/-}$ versus WT mice.

Click here to Download Table S1

Table S2. Enrichment of GO biological processes and KEGG pathways in LS-G6pc$^{-/-}$ mice with HCA versus LS-G6pc$^{-/-}$ mice without HCA.

Click here to Download Table S2

Table S3. Enrichment of GO biological processes and KEGG pathways LS-G6pc$^{-/-}$ mice with amyloidosis versus LS-G6pc$^{-/-}$ mice without amyloidosis.

Click here to Download Table S3

Table S4. Enrichment of GO biological processes and KEGG pathways in LS-G6pc$^{-/-}$ versus WT mice over time.

Click here to Download Table S4